Article

Chinese Science Bulletin

Astronomy

February 2011 Vol.56 No.4-5: 376–379
doi: 10.1007/s11434-010-4301-2

Preliminary results of FeO mapping using Imaging Interferometer data from Chang'E-1

LING ZongCheng[1,2*], ZHANG Jiang[1,2], LIU JianZhong[1], ZHANG WenXi[3], BIAN Wei[1], REN Xin[1], MU LingLi[1], LIU JianJun[1] & LI ChunLai[1]

[1] *National Astronomical Observatories, Chinese Academy of Sciences, Beijing 100012, China;*
[2] *School of Space Science and Physics & Shandong Provincial Key Laboratory of Optical Astronomy and Solar-Terrestrial Environment, Shandong University at Weihai, Weihai 264209, China;*
[3] *Academy of Opto-Electronics, Chinese Academy of Sciences, Beijing 100080, China*

Received September 29, 2010; accepted November 24, 2010

Information about the variability, and spatial distribution of iron abundance is important to understand lunar geological history and for future resource utilization. In this paper we present a preliminary model to produce an iron abundance map using images taken by an Imaging Interferometer on board the satellite Chang'E-1. Compared with the Clementine UVVIS images, the images from the Chang'E-1 satellite also allowed for the extraction of FeO abundance distributions on the Moon. However, the preliminary model results suggest an underestimation of ~2 wt.% for the FeO content of the mare region and an overestimation of ~3 wt.% for the highland region.

Chang'E-1, Imaging Interferometer, FeO mapping, Clementine UVVIS

Citation: Ling Z C, Zhang J, Liu J Z, et al. Preliminary results of FeO mapping using Imaging Interferometer data from Chang'E-1. Chinese Sci Bull, 2011, 56: 376–379, doi: 10.1007/s11434-010-4301-2

On March 1, 2009, China's first lunar probe, Chang'E-1 successfully impacted the Moon's surface at 52.36°E, 1.50°S near Mare Fecunditatis and completed 494 days of operation since launching on October 24, 2007. As one of eight scientific payloads on the Chang'E-1, an Imaging Interferometer (IIM) was used to detect the distribution of lunar chemical compositions and minerals on the Moon's surface [1]. The Vis-NIR reflectance properties of the Moon are sensitive to the mineralogy and physical states of the lunar regolith [2]. Information about the variability and spatial distribution of iron abundance is important to understand the petrogenesis of lunar rocks and thus the nature and origin of the Moon [3]. Many models have been suggested to extract iron abundance from Clementine's UVVIS images [3–9]. As more mission datasets (e.g. Kaguya (Japan), Chang'E-1 (China), Chandrayaan-1 (India) and the Lunar Reconnaissance Orbiter (United States)) [10] become available, a comparison of the results from these datasets as well as the refinement of the FeO mapping algorithm would be useful. In this paper, we present the preliminary results and produce an iron abundance map using the data from Chang'E-1 IIM.

1 Instrument and data overview

The IIM aboard the Chang'E-1 lunar probe was a Fourier transform Sagnac imaging spectrometer. It operated from the visible to the near infrared (0.48–0.96 μm) spectral region with 32 channels at spectral intervals of 325.5 cm^{-1}. The IIM was a push-broom imaging spectrometer with a 512×512 CCD detector to observe the Moon in polar orbit. In an orbit 200 km above the Moon, the Chang'E-1 IIM yielded a ground resolution of 200 m/pixel and a 25.6 km swath width. The main parameters of the IIM are shown in Table 1.

*Corresponding author (email: zcling@nao.cas.cn)

Table 1 Main IIM parameters

IIM parameters	Descriptions
Swath width	25.6 km
Ground resolution	200 m
Imaging coverage	between 75°S and 75°N
Spectral range	0.48–0.96 μm
Spectral channels	32 bands (for 0.48 μm, the band width is 7.62 nm; for 0.96 μm, the band width is 29 nm)
Digital level	12 bit
Pixel No.	256×256 (after 2×2 pixels combination)
MTF	≥0.2 (for quick-look mosaics)
S/N	≥100 (for quick-look mosaics when the lunar reflectance equals 0.2 and incidence angle equals 30°)
Electronic gain	3 types (1, 1.5, 2)
Exposure time	2 types (140 ms and 70 ms)
Frame rate	7.1 frame/s and 14.2 frame/s
Data rate	1406 kbps
Interferogram sampling mode	truncation sampling (default) and interval sampling

The IIM data was obtained from 84% of the Moon's surface area between latitudes of 70°S and 70°N. The IIM data underwent dark current and "flat-field" calibration, radiometric calibration (change in the raw digital number to radiance) and photometric as well as phase normalization (normalized to a standard geometry of i = 30°, e = 0°). The dark current level and the radiometric calibration coefficients for radiometric calibration were determined in the laboratory. We applied photometric calibration using a modified Lommel-Seelinger photometric model [11]. A homogeneous region near the Apollo 16 sampling site was chosen as the calibration target and laboratory spectrum from the mature lunar sample 62231 was used as a standard to calibrate the radiance values into absolute reflectance [12]. The data used in this work is level 2C after the above-mentioned calibrations.

2 Algorithm to derive FeO abundance

2.1 Clementine UVVIS method

Before Clementine, efforts to map the iron abundance on the moon were limited; however, it was suggested that an algorithm similar to the algorithms used for Ti mapping could be used [13,14]. Laboratory spectroscopic studies of lunar soils suggest that their reflectance decreases with an increase in nanophase Fe (and hence maturity) but the ratio of near-IR to visible reflectance increases (becomes "redder") [14]. Thus, in FeO mapping it is important to decouple the spectral effects of composition and maturity.

After obtaining data from Clementine, a series of empirical models were developed to predict the FeO content from Clementine's UVVIS images [3–9]. Among these models, Lucey's model is one of the most popular, following a series of refinements [7–9]. Lucey's model is based on the reflectance at 0.75 μm and the ratio of the reflectances at 0.95 μm and 0.75 μm. They found that the spectra of the obtained lunar samples (as well as from the Apollo and Luna sampling sites) had similar FeO compositions but varying maturity resulted in linear trends on a plot of NIR/Vis ratio versus the Vis reflectance. This trend is related to the FeO content and maturity. It has been suggested that these trends extend radially away from a theoretical hyper mature endmember and the angular spectral parameter θ_{Fe}. Based on the final processing of the Clementine UVVIS images, Lucey et al. [6] obtained the following algorithm to extract FeO abundance from the Clementine UVVIS data:

$$\theta_{Fe} = -\arctan\left(\frac{R_{891}/R_{757}-E}{R_{757}-F}\right),$$

$$\text{FeO wt.\%} = \theta_{Fe}\times 17.427 - 7.565.$$

In this paper, we used Lucey's model to validate the FeO model for the Chang'E-1 IIM data.

2.2 Chang'E-1 IIM method

The method used to calculate FeO abundance is similar to that of Lucey et al. [6]. Among the 32 bands of the IIM, five spectral channels (B23 (739 nm), B24 (757 nm), B30 (891 nm), B31 (918 nm) and B32 (947 nm)) are comparable to Clementine's two bands (750 and 950 nm) for the FeO model. We extracted average spectra consisting of 5×5 pixels from a relatively homogenous region from IIM orbit 2624 and compared its spectra with Clementine's UVVIS data (shown in Figure 1). Because of the limited response of the CCD detector, the 918 nm and 947 nm data were of poor quality. We thus used band B24 (757 nm) and B30 (891 nm) for the calculations and assumed that an analogous optical effect was present.

The first step was to acquire spectra for the Apollo and Luna sampling stations from the Chang'E-1 IIM data. Unfortunately, IIM missed the Apollo 15 site and thus we

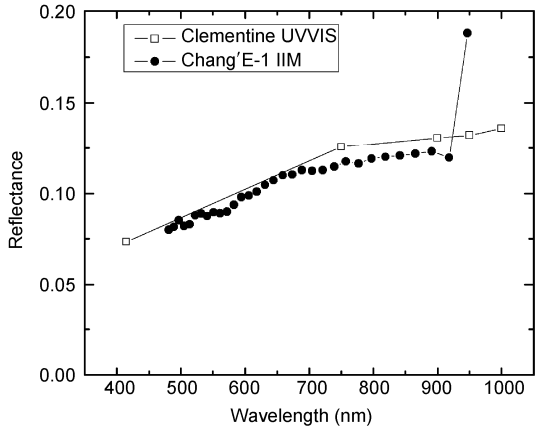

Figure 1 Average spectra of the homogeneous region in IIM orbit 2624 and the corresponding Clementine UVVIS spectra.

could only use the other 38 sampling sites from the Table of Lucey et al. [6] to derive the algorithm for the calculation of FeO content.

The chemical content of the sampled lunar soils from the Apollo and Luna missions are the "ground truth" for lunar studies. We tried to correlate the laboratory determined FeO content of typical lunar soils from the lunar landing sites with the remotely sensed image data. The spectral data for the 38 sample-returned sites and stations that were extracted from the Chang'E-1 images were plotted as a ratio-reflectance diagram, as shown in Figure 2. Calculations to suppress the maturity effect by the angle referred to as the Fe sensitive parameter θ_{Fe} are important and they have a linear relationship with FeO abundance. By maximizing the correlation between the remotely measured θ_{Fe} and the FeO content, we obtained a "hyper mature" endmember with an origin at (0.088, 1.548) and this yielded a correlation coefficient of 0.94.

We obtained the following expression for θ_{Fe}:

$$\theta_{\mathrm{Fe}} = -\arctan\left(\frac{R_{891}/R_{757}-1.548}{R_{757}-0.088}\right).$$

A plot of the station FeO content and the spectral iron parameter is shown in Figure 3. The best fit equation for these data points is

$$\mathrm{FeO\ wt.\%} = \theta_{\mathrm{Fe}} \times 43.394 - 50.952.$$

The scatter of the data points about the polynomial fit has a standard deviation of 1.58 wt.% FeO and this was estimated by the following formula:

$$\sqrt{\frac{\sum(\mathrm{FeO}_{\mathrm{predicted}}-\mathrm{FeO}_{\mathrm{real}})^2}{N-1}}.$$

The equation that we obtained is based on all the available Apollo and Luna sites from the IIM data and it is thus suitable for lunar global FeO mapping. However, in this study we concentrated on a regional case study to compare our model with Lucey's FeO model to refine our model.

3 Regional case study

Based on our model and the algorithm by Lucey [6], we produced a strip of an iron map near the southern rim of Mare Crisium (shown in Figure 4). We chose this region because it is on the boundary of the mare and the highland and thus a relatively complex material type can be expected.

When we compare these results with that obtained using Lucey's model, we found some similarities and a good correlation between the images. At first glance, the FeO map from Chang'E-1 seems to show more detail and texture than that from Clementine. This may be caused by an overestimation of FeO in the mare region. Chang'E-1's data seem to show an iron poor region with more detailed features in the mare regions. The highland regions are shown to be iron rich. The average FeO content difference between the two

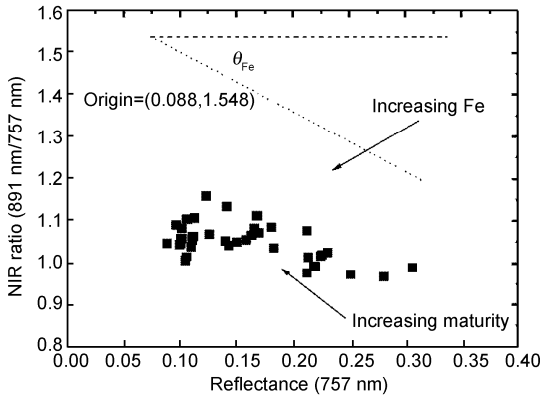

Figure 2 NIR ratio-reflectance plot for the sample-returned sites and the stations observed by the Chang'E-1 IIM.

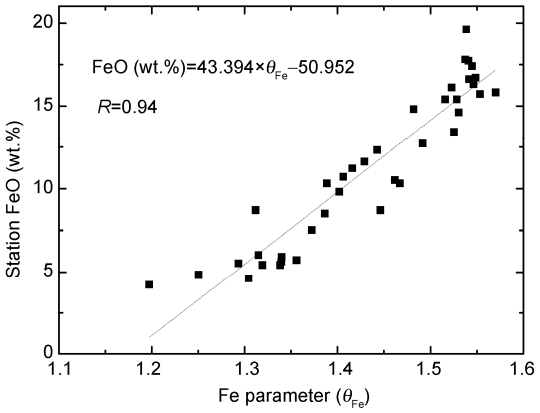

Figure 3 FeO content of the Apollo and Luna samples versus the spectral iron parameter θ_{Fe}.

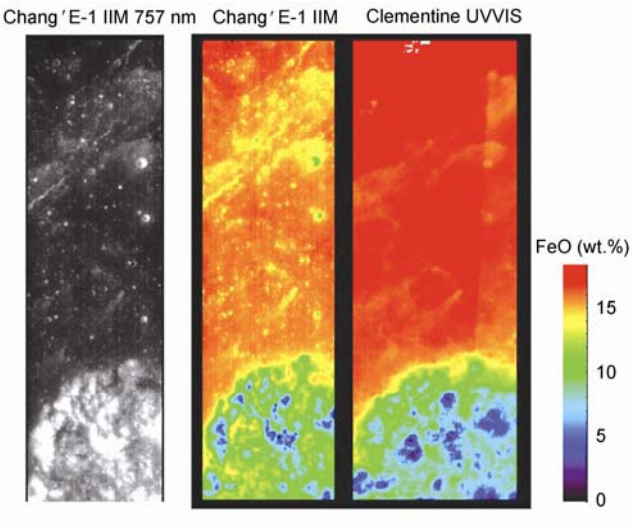

Figure 4 Comparison of the iron abundance map between the Chang'E-1 IIM and the Clementine UVVIS images.

images was 0.51 wt.% (14.07 wt.% for IIM and 14.58 wt.% for UVVIS). The distribution of the respective data points is shown in Figure 5. The bimodal distribution is in relation to the mare and highland regions. The major mare soil contains

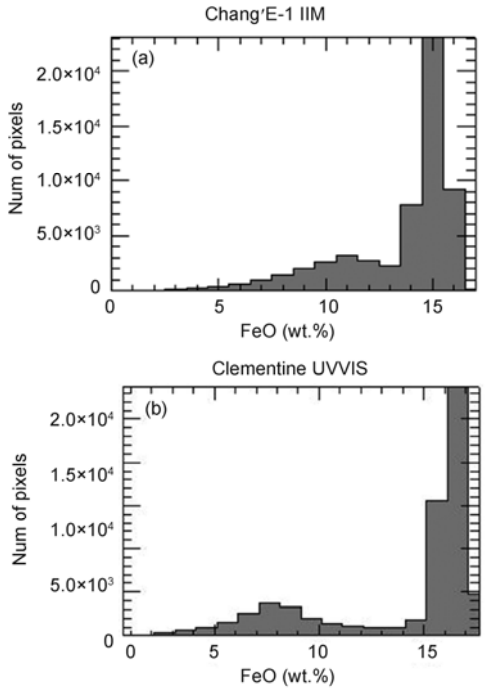

Figure 5 Data distributions of the Chang'E-1 IIM (a) and Clementine UVVIS (b) images.

16 wt.%–17 wt.% FeO while Chang'E-1 data show a peak at around 15 wt.%. Conversely, the Chang'E-1 data indicate a higher iron content (11 wt.%) in the highland compared with that from the Clementine data (8 wt.%–9 wt.%) and thus an overestimation of 3 wt.% was obtained.

The discrepancies in FeO content between these two images may be complex. First, we neglected the Apollo 15 data, which included different rock types (such as low Ti mare samples with different reflectance properties). Second, the absolute reflectance of the IIM data used in these calculations had a lower signal-to-noise ratio than that of the Clementine data. Third, because of the poor quality of the 918 and 947 nm images, we choose the band at 891 nm for the regression calculations (not the 950 nm as Lucey et al. did [6]). This may decrease the sensitivity of this model. In addition, because the two images have different solar incidence directions, a topographic shading effect may potentially cause a difference in the FeO content especially for the steep highland regions and some shaded craters in the mare region. Future work such as local topography corrections based on a digital elevation model with a similar resolution to that of the IIM data would improve the prediction results of our model.

4 Conclusions

We produced a preliminary algorithm for a FeO map model from Chang'E-1 IIM images. Compared with the Clementine UVVIS images, the IIM datasets from the Chang'E-1 satellite also have the potential to extract FeO abundance distributions of the Moon. The iron map derived by this model shows good correlations with the Clementine FeO map. However, preliminary model results suggest an underestimation (~2 wt.%) of the FeO content for the mare region while an overestimation (~3 wt.%) was obtained for the highland region. We will continue to investigate the origin of these discrepancies and errors in this algorithm to improve our FeO model.

This work was supported by the National High-Tech Research and Development Program of China (2008AA12A212/211/213), China Postdoctoral Science Foundation (20090450580), the National Natural Science Foundation of China (11003012) and the Young Researcher Grant of the National Astronomical Observatories, Chinese Academy of Sciences.

1 Zheng Y C, Ouyang Z Y, Li C L, et al. China's lunar exploration program: Present and future. Planet Space Sci, 2008, 56: 881–886
2 Lucey P G, Korotev R L, Gillis J J, et al. Understanding the lunar surface and space-Moon interactions. Rev Miner Geochem, 2006, 60: 83–219
3 Lucey P G, Taylor G J, Malaret E. Abundance and distribution of iron on the Moon. Science, 1995, 268: 1150–1153
4 Blewett D T, Lucey P G, Hawke B R, et al. Clementine images of the lunar sample-return stations: Refinement of FeO and TiO_2 mapping techniques. J Geophys Res, 1997, 102: 16319–16325
5 Lucey P G, Blewett D T, Hawke B R. Mapping the FeO and TiO_2 content of the lunar surface multispectral imagery. J Geophys Res, 1998, 103: 3679–3699
6 Lucey P G, Blewett D T, Jolliff B L. Lunar iron and titanium abundance algorithms based on final processing of Clementine ultraviolet-visible images. J Geophys Res, 2000, 105: 20297–20305
7 Lawrence D J, Feldman W C, Elphic R C, et al. Iron abundances on the lunar surface as measured by the lunar prospector gamma-ray and neutron spectrometers. J Geophys Res, 2002, 107: 5130
8 Gillis J J, Jolliff B L, Korotev R L. Lunar surface geochemistry: Global concentrations of Th, K, and FeO as derived from lunar prospector and Clementine data. Geochim Cosmochim Acta, 2004, 68: 3791–3805
9 Wilcox B B, Lucey P G, Gillis J J. Mapping iron in the lunar mare: An improved approach. J Geophys Res, 2005, 110: E11001
10 Pieters C M, Head J W, Isaacson P, et al. Lunar international science coordination/calibration targets (L-ISCT). Adv Space Res, 2008, 42: 248–258
11 Hillier J K, Buratti B J, Hill K. Multispectral photometry of the moon and absolute calibration of the Clementine UV/Vis camera. Icarus, 1999, 141: 205–225
12 Pieters C M. The Moon as a spectral calibration standard enabled by lunar samples: The Clementine example. Workshop on New Views of the Moon II, 1999, abstract #8025
13 Charette M P, Mccord T B, Pieters C M, et al. Application of remote spectral reflectance measurements to lunar geology classification and determination of titanium content of lunar soils. J Geophys Res, 1974, 79: 1605–1613
14 Fischer E M, Pieters C M. Remote determination of exposure degree and iron concentration of lunar soils using Vis-Nir spectroscopic methods. Icarus, 1994, 111: 475–488